Bone and Arthrosurgery Science, 2025, Volume 3, Issue 4
http://ojs.bbwpublisher.com/index.php/BAS
Online ISSN: 2981-8222
Print ISSN: 3083-4856

Analysis of Morphological Characteristics of Modic Changes in the Lumbar Spine Based on MRI Imaging Omics and Their Association with Low Back Pain

Tuanmao Guo[1], Yuan Xiao[1], Yanli Xing[2]*

[1]Department of Orthopaedics, Xianyang Central Hospital, Xianyang 712000, Shaanxi, China
[2]Department of Pharmacy, Xianyang Central Hospital, Xianyang 712000, Shaanxi, China

**Author to whom correspondence should be addressed.*

***A*bstract:** *Objective*: To analyse the MRI imaging characteristics, morphological features, and association with low back pain in different types of Modic changes (MC) of the lumbar spine. Features in different types of Modic changes (MC) in the lumbar spine and their association with low back pain. *Methods*: A retrospective analysis was conducted on the clinical data of 124 patients who underwent lumbar MRI examinations and were diagnosed with Modic changes between March 2024 and February 2025 at a certain hospital. Prospective collection of imaging and clinical data was conducted on 30 patients with different types of lumbar Modic changes and low back pain scores during the same period. Pyradiomics was used to extract MRI morphological and radiomics features in Modic changes, followed by Kruskal-Wallis test, Dunn's test, Mann-Whitney U test, correlation analysis, LASSO regression screening, and validation of differential features. A classification model was constructed using the support vector machine (SVM) algorithm, and heatmap analysis was performed to investigate the correlation between MRI morphological and radiomics features and low back pain scores. *Results*: Among 154 patients without low back pain, 34 were Modic Type I, 62 were Type II, and 58 patients with Modic Type III. A total of 7 morphological features and 19 radiomics features showed significant differences in mean values among the three Modic groups ($P < 0.05$). A Modic classification model based on the differential features was constructed using SVM, with an accuracy rate of 98%. In the correlation analysis, ODI scores were positively correlated with the long-to-short axis ratio and surface area-to-volume ratio of morphological features, and negatively correlated with sphericity and flatness ($P < 0.05$). Additionally, it was positively correlated with the radiomics feature FS_lbp_3D_m1_glszm_ZoneEntropy (r = 0.380, $p < 0.05$) and negatively correlated with T1_lbp_3D_m2_glszm_SmallAreaLowGrayLevelEmphasis (r = -0.423, $p < 0.05$) and FS_wavelet_LLH_firstorder_90thPercentile (r = -0.376, p < 0.05). *Conclusion*: Morphological and radiomics features differ among different subtypes of Modic changes (MC). An automatic classification model constructed based on these differential features demonstrates high accuracy, and key features are significantly associated with the low back pain functional disability index.

Keywords: Low back pain; Modic changes; Radiomics; Machine learning

Online publication: August 29, 2025

1. Introduction

Modic changes (MC) in the lumbar spine are characteristic signal abnormalities of the vertebral endplates and adjacent bone marrow on MRI, and are independent risk factors for severe and disabling low back pain. Although studies have shown that Type I MC is significantly associated with nonspecific chronic low back pain, the exact pathological mechanisms and specific associations with pain severity remain unclear. Current studies primarily focus on the presence, classification, and area of MCs, lacking precise quantitative analysis of lesion morphological characteristics, which limits a deeper understanding of the pathological progression of MCs and their pain-inducing mechanisms [1]. In recent years, the emergence of radiomics has provided a powerful tool for in-depth analysis of medical images. It can high-throughput extract and quantify features such as texture, shape, and intensity distribution that are difficult to identify with the naked eye, thereby revealing potential pathological information. However, there are no studies investigating the morphological differences of lumbar MC using radiomics and exploring the association between these quantitative features and clinical symptoms of low back pain. Given this, the present study aimed to utilise radiomics methods based on conventional MRI sequences of the lumbar spine (T1WI, T2WI, FS), to precisely extract and quantitatively analyse morphological features of lesion regions in different types of MC (Type I vs. Type II). By analysing the relationship between cases where HIZ and Modic changes coexist on MRI and the occurrence of provoked consistent pain, and evaluating the specificity and sensitivity of combining these two features as a diagnostic marker, this study aims to establish a reliable and practical diagnostic method for DLBP [2]. Additionally, by analysing the pathological changes in different regions of degenerative intervertebral discs represented by the HIZ zone and Modic signs, and combining these findings to study their relationship with DLBP, this study aims to deepen the understanding of the morphological characteristics of MC and its association with low back pain from an imaging quantitative perspective, thereby providing new imaging evidence for exploring the pathological mechanisms and potential therapeutic targets of MC-related low back pain.

2. Materials and methods

2.1. General data

A retrospective analysis was conducted on MRI data from 124 patients with lumbar Modic changes diagnosed between March 2024 and February 2025 at our hospital. Concurrently, 30 patients with lumbar Modic changes of different types and low back pain scores were prospectively enrolled, and their imaging and clinical data were collected. Imaging features were analysed to investigate their association with low back pain scores.

Inclusion criteria: (1) Confirmed Modic changes (Types I–III) by lumbar MRI; (2) Age 18–70 years old, no gender restrictions; (3) Complete T1WI, T2WI, and FS sequence imaging data.

Exclusion criteria: (1) Concurrent vertebral fractures, tumours, infections, or prior lumbar spine surgery; (2) Severe spinal stenosis (sagittal diameter ≤ 10 mm) or nerve root compression causing lower extremity radicular pain; (3) Incomplete key clinical data (e.g., classification records, pain scores) or damaged imaging data; (4) Patients with concomitant rheumatic immune diseases, metabolic bone diseases, congenital lumbar abnormalities, or scoliosis.

2.2. Methods

2.2.1. Modic change classification diagnosis

Assess the type of Modic changes in patients according to the diagnostic criteria for Modic changes in the lumbar

spine, excluding degenerative or infectious secondary changes: Type I: Low signal intensity on T1-weighted images (T1WI) of the endplates and adjacent bone, and high signal intensity on T2-weighted images (T2WI); Type II: High signal intensity on T1WI, and equal/slightly higher signal intensity on T2WI; Type III: Low signal intensity on both T1WI and T2WI.

2.2.2. Grading of lumbar disc degeneration and pain scoring

The degree of degeneration of Modic changes was assessed using the Pfirrmann criteria on T2WI sagittal images of lumbar MRI. Grade I-II was considered normal, and grades III-V corresponded to mild, moderate, and severe degeneration, respectively. The Oswestry Disability Index (ODI) and Visual Analogue Scale (VAS) were used to evaluate low back pain in 30 prospectively enrolled patients. The ODI assesses 10 dimensions of pain intensity, activities of daily living, lifting, walking, sitting, standing, sleep disturbance, sexual activity, social activity, and travel, with each item scored 0–5; VAS assessed pain intensity using a 10-cm scale (0 cm no pain, 10 cm severe pain), with continuous variables supporting parametric tests.

2.2.3. MRI normalisation and ROI segmentation

To eliminate the influence of different scanning devices, all MRI data were subjected to signal intensity normalization. Subsequently, using ITK-SNAP software, regions of interest (ROIs) were delineated on T1-weighted images (T1WI), T2-weighted images (T2WI), and fat-suppressed (FS) sequences for Modic lesions. Given that Modic changes often involve adjacent vertebrae, the ROI was defined within a single spinal functional unit containing the visible lesion and annotated on consecutive cross-sectional images across all relevant sequences. Cases with preliminary ROI delineation were reviewed by another senior physician with over ten years of clinical experience.

2.2.4. Imageomics feature extraction

Using the Python (v3.9.13) platform, the PyRadiomics toolkit is used to extract radiomics features from ITK-SNAP-annotated ROIs. A total of 107 quantitative parameters are calculated from each raw image, including first-order statistics, morphological features, and texture metrics based on the grey-co-occurrence matrix, grey-distance matrix, grey-size matrix, grey-dependence matrix, and adjacent grey-difference matrix. To enhance the information content of the features, filtering techniques were applied prior to feature extraction to strengthen the structural and textural pattern recognition of the ROI regions.

2.3. Statistical analysis

(1) Statistical distribution of morphological features in different types of Modic changes

All features extracted from the original and filtered images were standardised based on the distribution of imaging features (morphology, intensity, texture, etc.) with significant differences across various Modic changes. A Mann-Whitney U test ($p < 0.05$) was then used for preliminary screening. Subsequently, correlation analysis was performed on the screened features, and redundant features with high correlation ($r > 0.9$) were removed. We then applied the LASSO algorithm to calculate the coefficients of the remaining features, retaining those with non-zero coefficients as key differential features. Based on these features, we constructed machine learning classification models and further analysed their descriptive statistical differences (mean/variance) across different Modic types and their correlations with clinical baseline data.

(2) Statistical analysis of the distribution of imaging features among different Modic types

First, standardise the features extracted from the original and filtered images, and perform a Mann-Whitney U test ($p < 0.05$) to screen the features. Then, perform a correlation analysis on the screened features, remove redundant features with high correlation ($r > 0.9$), and apply the LASSO algorithm to calculate the coefficients of the remaining features, retaining the features with non-zero coefficients as the key difference feature set. Finally, a machine learning classification model is constructed based on this feature set to comprehensively evaluate the descriptive statistical differences (mean/variance) between different Modic types and their correlation with clinical baseline data.

3. Results

3.1. Baseline data

This study included 154 participants, including 124 without low back pain scores (88 males, 36 females), aged 18–70 years old, with an average age of 58.36 ± 5.10 years old. Among them, 34 were Modic Type I, 62 were Type II, and 28 were Type III; Among the 30 participants with low back pain scores prospectively collected, there were 7 males and 23 females, aged 19–71 years, with a mean age of 56.80 ± 6.62 years old. Among these, 7 were Modic Type I, 22 were Type II, and 1 was Type III. Due to the single case of Type III in the prospective cohort, its mean characteristics were not included in subsequent statistical analyses.

3.2. Morphological characteristics distribution of different modic types

Fifteen shape features were extracted from the ROI of T2WI images using PyRadiomics (**Table 1**). This table shows the mean (standard deviation) distribution of features in each Modic type, with means (SD) marked with "*" indicating that the feature followed a normal distribution in the corresponding type ($P < 0.05$). Kruskal-Wallis (KW) non-parametric tests were used to analyse intergroup differences, identifying seven morphological features with statistically significant differences ($P < 0.05$): elongation ($P = 0.000074$), flatness ($P = 0.014935$), major axis length (MajorAxisLength, $P = 0.030619$), major axis length to minor axis length ratio (MajorAxisLength/LeastAxisLength, $P = 0.014935$), axial maximum two-dimensional diameter (Maximum 2D Diameter Slice, $P = 0.022303$), sphericity (Sphericity, $P = 0.000012$), and surface area-to-volume ratio (Surface Volume Ratio, $P = 0.000010$).

Table 1. Distribution of Modic change morphological characteristics and KW test results for different subtypes

Feature	Mean (SD)			Difference Test (Kw test)
	Type I	Type II	Type III	
Elongation	0.816 (0.112)*	0.736 (0.124)	0.779 (0.111)	0.000074*
Flatness	0.629 (0.137)	0.575 (0.120)	0.609 (0.119)	0.014935*
Short axis ratio	25.259 (5.955)	24.620 (5.348)	24.956 (6.093)	0.774269
Major axis length	40.380(6.273)	43.425(8.399)	41.246 (7.495)	0.030619*
Long axis ratio	1.677 (0.416)*	1.835 (0.522)*	1.708 (0.348)	0.014935*
Maximum two-dimensional diameter (column direction)	44.065 (7.279)	46.258 (8.276)*	47.270 (8.102)	0.101193
Maximum two-dimensional diameter (row direction)	41.004 (8.084)	42.466(9.395)*	41.448 (9.250)	0.265319
Maximum two-dimensional diameter (axial)	40.312 (5.108)	39.012 (5.265)*	41.577 (5.597)*	0.022303*

Table 1 (Continued)

Feature	Mean (SD)			Difference Test (Kw test)
	Type I	Type II	Type III	
Maximum three-dimensional diameter	47.887 (7.108)	49.467 (7.981)	50.200 (8.074)	0.247682
Grid volume	12,226.669 (6,490.95)	10521.627 (5558.275)*	14,321.675 (9,160.341)	0.052316
Short axis length	32.596 (4.924)	31.306 (4.976)	31.774 (5.746)	0.333330
Spherical degree	0.438 (0.039)	0.405 (0.053)*	0.424 (0.045)	0.000012*
Surface area	5744.109 (2251.073)	5684.179 (2152.712)*	6473.510(2559.349)	0.348311
Surface area to volume ratio	0.520(0.116)*	0.592(0.124)	0.515 (0.116)	0.000010*
Voxel volume	12,416.356 (6,515.319)	10705.479 (5581.332)*	14,521.310 (9,205.617)	0.054961

To identify the specific intergroup differences among the seven morphometric features that showed overall significance in the Kruskal-Wallis test, Dunn's post hoc test was used for pairwise comparisons (**Table 2**). The analysis revealed that elongation rate, flatness, sphericity, surface area-to-volume ratio, and long-to-short axis ratio all exhibited statistically significant differences between Modic I and Modic II types. The surface area-to-volume ratio showed significant differences not only between Modic I and II types but also between Modic II and III types ($P < 0.05$). The long axis length and axial maximum two-dimensional diameter did not reach statistical significance ($P > 0.05$), but their *P*-values were close to the critical level. The Kruskal-Wallis test, as a non-parametric method, may be limited in effectiveness when sample sizes are small or the population distribution deviates from the assumption, and it is prone to outliers, leading to false positives. In contrast, Dunn's Test exhibits greater robustness, particularly for comparisons between small sample groups. The reason for this may be that the two features (long axis length and maximum two-dimensional diameter) exhibited marginal significance in the overall test (KW $P < 0.05$).

Table 2. Results of Dunn's Test for morphological features with significant differences

Features with significant differences	Dunn's Test results			
Elongation rate	P-value	1	2	3
Elongation	1	1.000000	0.000079	0.431213
	2	0.000079*	1.00000	0.180102
	3	0.431213	0.180102	1.000000
Flatness	P-value	1	2	3
Flatness	1	1.000000	0.018587	1.0000
	2	0.018587*	1.00000	0.46437
	3	1.000000	0.46437	1.00000
Long axis length	P-value	1	2	3
	1	1.000000	0.051191	1.000000
	2	0.051191	1.00000	0.375196
	3	1.000000	0.375196	1.000000

Table 2 (Continued)

Features with significant differences	Dunn's Test results			
Maximum two-dimensional diameter (axial)	P-value	1	2	3
	1	1.000000	0.178804	1.000000
	2	0.178804	1.000000	0.062015
	3	1.000000	0.062015	1.000000
Sphericity	P-value	1	2	3
	1	1.000000	0.000022	0.601980
	2	0.000022*	1.0000	0.057642
	3	0.601980	0.057642	1.00000
Surface area to volume ratio	P-value	1	2	3
	1	1.000000	0.000154	1.000000
	2	0.000154*		0.003347
	3	1.0000	0.003347*	1.000000
Long-to-short axis ratio	P-value	1	2	3
	1	1.000000	0.018587	1.0000
	2	0.018587*	1.0000	0.46437
	3	1.000000	0.46437	1.0000

3.2. Imagingomics differences in Modic changes of different types

Radiomics features were extracted from T1WI, T2WI, and FS sequences using PyRadiomics. Compared with a single sequence, the combination of T1WI+T2WI+FS significantly improved the accuracy of Modic classification. The feature extraction process includes raw images and seven types of transformation processing: wavelet, Gaussian-Laplace filtering (LoG), pixel square (Square), square root of intensity (SquareRoot), logarithmic transformation (Logarithm), exponential transformation (Exponential), local binary pattern (LocalBinaryPattern2D/3D), and gradient features (Gradient). Each sequence extracts 1,906 features. To screen for Modic classification-specific features, the following screening criteria are applied:

(1) Mean-centred and variance-scaled the original data (mean = 0, variance = 1);

(2) The standardised features were analysed using the Mann-Whitney U test to screen out 1,336 features with significant intergroup differences ($P < 0.05$). Their distribution relative to the threshold line ($P = 0.05$) is shown in the scatter plot in **Figure 1**. The points in **Figure 1** represent the features extracted from different image types, and the red horizontal line indicates the critical condition of $P = 0.05$.

(3) Highly correlated features ($r > 0.9$) were removed, prioritising variables with the highest average absolute correlation, resulting in 823 features retained;

(4) The LASSO algorithm (optimal alpha = 0.044984) was used to calculate feature coefficients (**Figure 2**) and screen non-zero coefficient features.

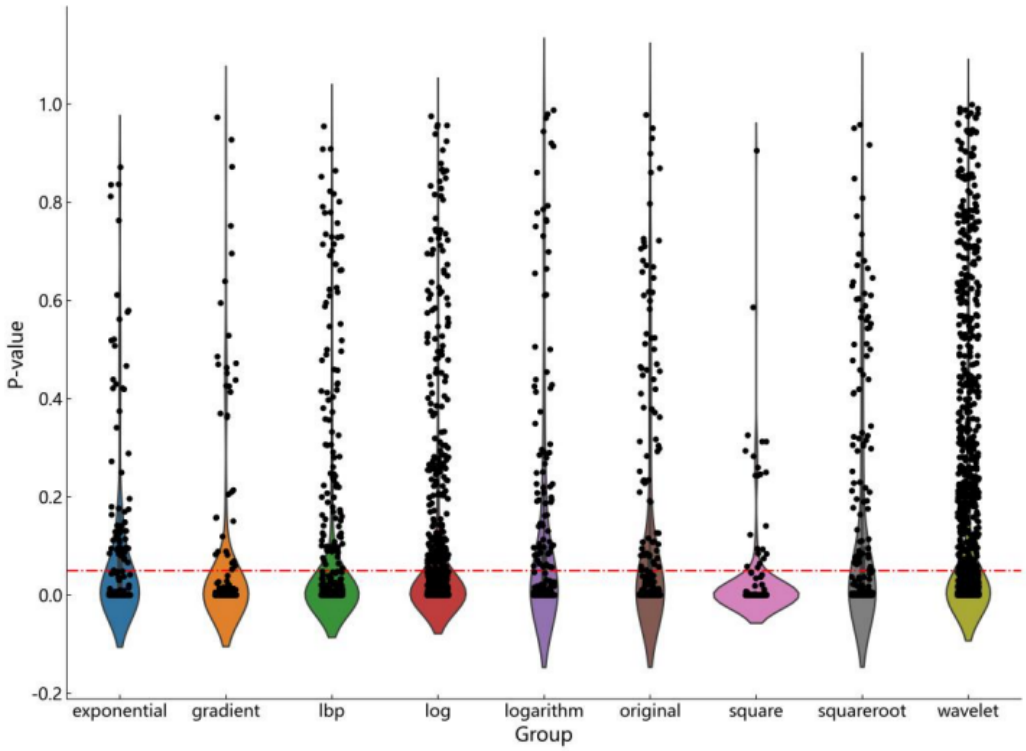

Figure 1. Mann-Whitney U test results.

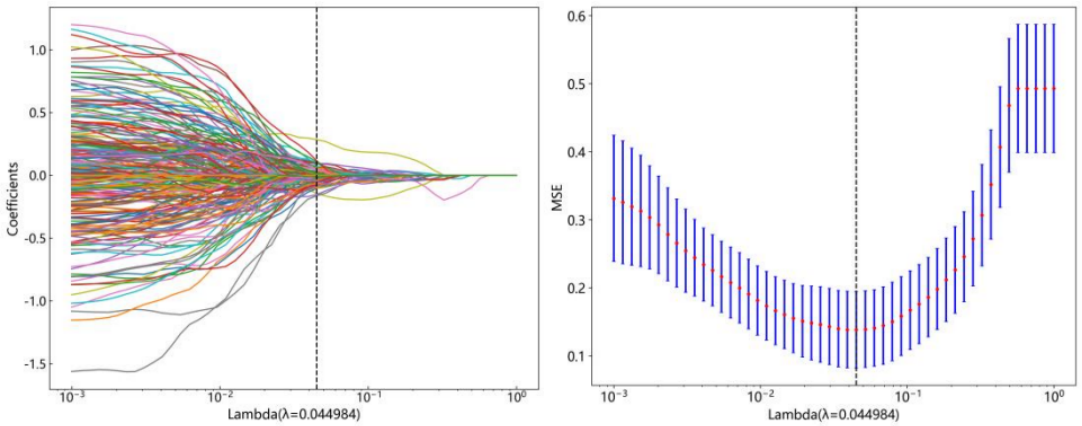

Figure 2. LASSO regression coefficient distribution plot.

Based on the 29 non-zero coefficient features selected by LASSO (threshold > 1×10^{-6}), a Modic classification model was constructed using support vector machines (SVM). The model validation set achieved an accuracy rate of 98%, confirming that the selected features have significant discriminative efficacy for Modic classification. Further analysis using Kruskal-Wallis test and Dunn's test validated the differences between feature groups. The results showed that 15 features in the T1WI sequence exhibited significant intergroup differences ($P < 0.05$); 8 features in the T2WI sequence exhibited significant intergroup differences ($P < 0.05$); and 6 features in the FS sequence exhibited significant intergroup differences ($P < 0.05$). All 29 features reached a significant level in the Kruskal-Wallis test.

3.3. Correlation between radiomics features and low back pain

In this section, we used R language to analyse the correlation between the low back pain scores of the 30 patients prospectively collected and the aforementioned morphological and radiomic features. During the correlation analysis, since only 1 case in the prospectively collected cases belonged to Modic Type III, we only analysed data from Modic Type I and Modic Type II cases.

3.3.1. Correlation between morphological characteristics and low back pain

The study found that the Oswestry Disability Index (ODI) score was significantly correlated with specific lumbar morphological features. ODI was significantly positively correlated with the muscle fibre long-short axis ratio ($r = 0.391$, $p < 0.05$) and the surface area-to-volume ratio ($r = 0.506$, $p < 0.01$). Conversely, ODI scores were significantly negatively correlated with sphericity ($r = -0.499$, $p < 0.01$) and flatness ($r = -0.390$, $p < 0.05$). This indicates that elongated muscle fibre morphology, increased surface complexity, and deviation from spherical and flat states are associated with increased severity of low back pain.

3.3.2. Correlation between imaging group differences and low back pain

Research has found that the Oswestry Disability Index (ODI) score is significantly associated with specific radiological imaging features. ODI is positively correlated with the regional entropy of three-dimensional images from FS sequences (FS_lbp_3D_m1_glszm_ZoneEntropy, $r = 0.380$, $p < 0.05$); while it was negatively correlated with the low-greyscale small-area distribution in T1 sequences (T1_lbp_3D_m2_glszm_SmallAreaLowGrayLevelEmphasis, $r = -0.423$, $p < 0.05$) and the LLH wavelet 90th percentile (FS_wavelet_LLH_firstorder_90Percentile, $r = -0.376$, $p < 0.05$). Additionally, age is negatively correlated with the pixel grey level variability of the T2 sequence (T2_logarithm_firstorder_RobustMeanAbsoluteDeviation, $r = -0.390$, $p < 0.05$); while it was positively correlated with the uniformity of grey-level spatial distribution in the T1 sequence (T1_exponential_glszm_SizeZoneNonUniformityNormalized, $r = 0.492$, $p < 0.01$) and low grey-level large dependence (T1_lbp_3D_m1_gldm_LargeDependenceLowGrayLevelEmphasis, $r = 0.395$, $p < 0.05$).

4. Discussion

Modic changes are an independent risk factor for severe disabling low back pain [3]. This study investigated the morphological and radiomic features of lumbar MCs and their association with low back pain through quantitative analysis. The baseline characteristics of the study population were consistent with the incidence patterns of MCs and previous studies [4]. This study systematically revealed the imaging feature differences among MC subtypes for the first time: MC Type I exhibits higher elongation rate, flatness, and sphericity in morphology, suggesting a more spherical shape and flatter surface, which may be associated with its more active inflammatory state [5]; whereas MC Type II exhibits a larger major axis length, major-to-minor axis ratio, and surface area-to-volume ratio, with a morphology tending toward elongated or irregular shapes. The larger surface area-to-volume ratio may be associated with tissue swelling and deformation caused by inflammation [6], and this feature shows a significant positive correlation with the Oswestry Disability Index (ODI) ($r = 0.506$, $p < 0.01$); Additionally, ODI was positively correlated with the long-to-short axis ratio ($r = 0.391$, $p < 0.05$) and negatively correlated with sphericity ($r = -0.499$, $p < 0.01$) and flatness ($r = -0.390$, $p < 0.05$), indicating that elongated lesion morphology, surface complexity, and deviation from spherical and flat states are significantly associated with worsening low back pain severity.

Imageomics analysis further revealed that ODI was positively correlated with FS sequence regional entropy (FS_lbp_3D_m1_glszm_ZoneEntropy, r = 0.380, $p < 0.05$), while negatively correlated with the distribution of low-grayscale small regions in the T1 sequence (T1_lbp_3D_m2_glszm_SmallAreaLowGrayLevelEmphasis, r = -0.423, $p < 0.05$) and the FS sequence LLH wavelet 90th percentile (FS_wavelet-LLH_firstorder_90thPercentile, r = -0.376, $p < 0.05$). Reduced smoothness and increased regional entropy may be associated with oedema signals in the lesion, thereby influencing pain [7,8]. Additionally, age was significantly correlated with specific radiomic features: negatively correlated with pixel grey-scale variability in the T2 sequence (T2_logarithm_firstorder_RobustMeanAbsoluteDeviation, r = -0.390, $p < 0.05$); with the uniformity of grey-level spatial distribution in the T1 sequence (T1_exponential_glszm_SizeZoneNonUniformityNormalized, r = 0.492, $p < 0.01$) and the low grey-level large dependence (T1_lbp_3D_m1_gldm_LargeDependenceLowGrayLevelEmphasis, r = 0.395, $p < 0.05$), indicating that the texture and grey-level characteristics of lesion tissues change with age, supporting the role of age in the onset of MC [9]. A diagnostic model constructed using 29 significantly different radiomics features selected from T1 (15), T2 (8), and FS (6) sequences effectively distinguished MC subtypes, highlighting the diagnostic value of the T1WI sequence [10]. The innovation of this study lies in the first application of radiomics technology to quantitatively analyse MC characteristics and construct an automatic classification model, providing new insights into the pathogenesis of MC and the differentiation of MC-related low back pain.

5. Conclusion

The study demonstrates that morphological and radiomics features effectively differentiate between subtypes of Modic changes (MC). An automated classification model leveraging these discriminative features achieves high accuracy, with key features showing significant correlations with the low back pain functional disability index. These findings highlight the potential of radiomics-based approaches in improving MC subtype characterization and their clinical relevance in assessing functional disability. Further validation in larger cohorts could enhance the model's utility in personalized diagnosis and management.

Funding

Key Laboratory of Spinal Degenerative Diseases, Xianyang City (Project No.: L2023-CXNL-CXPT-ZDSYS-010); Key Technology Innovation Team Project for Minimally Invasive Spinal Surgery, Xianyang City (Project No.: L2022CXNLTD002); University-level Scientific Research Project, Shaanxi University of Traditional Chinese Medicine (Project No.: 2020FS06)

Disclosure statement

The authors declare no conflict of interest.

References

[1] Han Z, Kang X, Wei Y, et al., 2019, Differential Diagnosis of Modic Type I Changes in Lumbar MRI Examinations. Medical and Health Equipment, 40(10): 57–61 + 78.

[2] Zhu S, 2019, Distribution Characteristics and Associated Factors of Modic Changes in Patients With Low Back Pain,

thesis, Southwest Medical University.

[3] Buchbinder R, Underwood M, Hartvigsen J, et al., 2020, The Lancet Series Call to Action to Reduce Low Value Care for Low Back Pain: An Update. Pain, 161 Suppl 1(1): S57–S64.

[4] Peng Q, Yang S, Meng B, et al., 2024, Analysis of Intervertebral Disc Vacuum Phenomenon in Patients With Low Back Pain: A Retrospective Analysis of 298 Cases. Chinese Journal of Spine and Spinal Cord, 34(8): 826–833.

[5] Wang Y, Zhang H, Yao J, et al., 2025, Clinical Significance of Abnormal MRI Findings of Lumbar Facet Joints in Patients With Low Back Pain. Imaging Research and Medical Applications, 9(10): 134–136.

[6] Liu C, Yang H, Yang J, et al., 2025, Comparison of MRI Parameters Between Patients With Lumbar Instability and Stable Low Back Pain. Chinese Journal of Orthopaedic Surgery, 33(5): 468–472.

[7] Yan J, Huang Y, Liu X, et al., 2025, A Study on the Correlation Between Modic Changes in the Lumbar Spine and Disc Degeneration in Patients With Chronic Low Back Pain. Journal of Clinical Radiology, 44(1): 150–154.

[8] Conger A, Burnham T, Clark T, et al., 2022, The Effectiveness of Intraosseous Basivertebral Nerve Radiofrequency Ablation for the Treatment of Vertebrogenic Low Back Pain: An Updated Systematic Review With Single-Arm Meta-analysis. Pain Medicine, 23(Suppl 2): S50–S62.

[9] Yu T, Li N, Gao X, et al., 2024, The Value of Prone MRI in Diagnosing Low Back Pain and Refractory Radiculopathy in Patients With Lumbar Spine Disorders. Chinese Journal of CT and MRI, 22(12): 175–177.

[10] Shi N, Song H, Cao L, et al., 2024, The Association Between Modic Changes in the Lumbar Spine and the Volume and Morphology of Endplate Defects, and Their Correlation With Low Back Pain. Chinese Journal of Spine and Spinal Cord, 34(07): 711–718.